Mechanism of the Family 1 β-Glucosidase from *Streptomyces* sp: Catalytic Residues and Kinetic Studies†

Miquel Vallmitjana,‡ Mario Ferrer-Navarro,‡ Raquel Planell,‡ Mireia Abel,§ Cristina Ausín,§ Enrique Querol,‡ Antoni Planas,*,§ and Josep-Anton Pérez-Pons*,‡

Institut de Biologia Fonamental "Vicent Villar i Palasí" and Dept Bioquímica i Biologia Molecular, Universitat Autònoma de Barcelona, 08193 Barcelona, Spain, and Laboratory of Biochemistry, Institut Químic de Sarrià, Universitat Ramon Llull, 08017 Barcelona, Spain

Received December 27, 2000; Revised Manuscript Received February 28, 2001

ABSTRACT: The *Streptomyces* sp. β-glucosidase (Bgl3) is a retaining glycosidase that belongs to family 1 glycosyl hydrolases. Steady-state kinetics with *p*-nitrophenyl β-D-glycosides revealed that the highest k_{cat}/K_M values are obtained with glucoside (with strong substrate inhibition) and fucoside (with no substrate inhibition) substrates and that Bgl3 has 10-fold glucosidase over galactosidase activity. Reactivity studies by means of a Hammett analysis using a series of substituted aryl β-glucosides gave a biphasic plot log k_{cat} vs pK_a of the phenol aglycon: a linear region with a slope of $\beta_{lg} = -0.8$ for the less reactive substrates (p$K_a > 8$) and no significant dependence for activated substrates (p$K_a < 8$). Thus, according to the two-step mechanism of retaining glycosidases, formation of the glycosyl-enzyme intermediate is rate limiting for the former substrates, while hydrolysis of the intermediate is for the latter. To identify key catalytic residues and on the basis of sequence similarity to other family 1 β-glucosidases, glutamic acids 178 and 383 were changed to glutamine and alanine by site-directed mutagenesis. Mutation of Glu178 to Gln and Ala yielded enzymes with 250- and 3500-fold reduction in their catalytic efficiencies, whereas larger reduction (10^5-10^6-fold) were obtained for mutants at Glu383. The functional role of both residues was probed by a chemical rescue methodology based on activation of the inactive Ala mutants by azide as exogenous nucleophile. The E178A mutant yielded the β-glucosyl azide adduct (by ^{1}H NMR) with a 200-fold increase on k_{cat} for the 2,4-dinitrophenyl glucoside but constant k_{cat}/K_M on azide concentration. On the other hand, the E383A mutant with the same substrate gave the α-glucosyl azide product and a 100-fold increase in k_{cat} at 1 M azide. In conclusion, Glu178 is the general acid/base catalyst and Glu383 the catalytic nucleophile. The results presented here indicate that Bgl3 β-glucosidase displays kinetic and mechanistic properties similar to other family 1 enzymes analyzed so far. Subtle differences in behavior would lie in the fine and specific architecture of their respective active sites.

The Bgl3 β-glucosidase (β-glucoside glucohydrolase, EC 3.2.1.21) from *Streptomyces* sp. QM-B814 is a retaining glycosidase showing an exo-like action pattern by releasing glucose units from the nonreducing end of different β-linked disaccharides and oligosaccharides (*1*). Like other retaining glycosidases, the Bgl3 enzyme is able to perform very efficiently transglycosylation reactions (i.e., transfer of glycosidic residues), catalyzing the formation of β-1,4 or β-1,3 bonds depending on the acceptor (*2*). By means of ^{1}H NMR TR-NOE studies it was also determined that *Streptomyces* glucosidase recognizes and bounds only one of the three conformers of thiocellobiose, an analogue of cellobiose which behaves as a competitive inhibitor, in free solution (*3*). Following these structural aims, the protein has been crystallized (*4*), and the 3D structure resolution of its native form and complexes with nonhydrolyzable substrate analogues is currently undertaken (Guasch et al., manuscript in preparation).

In recent years a vast amount of mechanistic information on the enzymatic action of retaining glycosidases has been produced through mutagenesis, enzyme kinetics, inhibition, and X-ray crystallography studies (for reviews see refs *5*−*7*). On the basis of amino acid sequence similarities (*8*), glycosidases have been classified in more that 80 families (CAZY: *ca*rbohydrate-active enzymes at http://afmb.cnrs-mrs.fr/~pedro/CAZY/db.html). Enzymes belonging to the same family seem to share common mechanistic features, but given the large number of sequences and protein structures, subtle differences in the fine-tuning of the enzyme activity are expected, thus demanding detailed structural, kinetic, and mechanistic studies of a larger number of glycosidases to evaluate their particular molecular mechanisms.

From a mechanistic point of view, the transfer of glucosyl groups between oxygen nucleophiles catalyzed by β-glucosidases acting with retention of anomeric configuration is

† This work was supported by the Ministerio de Educación y Ciencia (Grants BIO97-0511-C02 and BIO2000-0647-C02 to E.Q. and A.P.) and the Generalitat de Catalunya [Centre de Referència en Biotecnologia (CERBA) to E.Q. and Grup Consolidad GQBB, ref 1999SGR 00335, to A.P.]. M.V. is the recipient of a predoctoral scholarship from CERBA.

* Corresponding authors. A.P.: tel, +34-932038900; fax, +34-932056266; e-mail, aplan@iqs.es. J.-A.P.-P.: tel, +34-935811331; fax, +34-935812011; e-mail, japerez@servet.uab.es.

‡ Universitat Autònoma de Barcelona.

§ Universitat Ramon Llull.

10.1021/bi002947j CCC: $20.00
Published on Web 04/26/2001

done by means of a double displacement mechanism through the formation of a covalent glycosyl-enzyme intermediate (*5*, *9*). For such a mechanism, two carboxylate residues are generally involved at the enzyme active site: one of them would act as the nucleophile, attacking the anomeric center of the substrate and displacing the leaving group to form the covalent intermediate, and the other as the general acid/base catalyst, providing protonic/deprotonating assistance for the release of the leaving group and the further attack of a water molecule on the covalent intermediate. For family 1 glycosyl hydrolases (*8*), nucleophile and general acid/base residues have been identified by site-directed mutagenesis in the β-glucosidases Abg from *Agrobacterium faecalis* and SSβ-gly from *Sulfolobus solfataricu*s as Glu358 and Glu170, respectively, for the former enzyme (*10*, *11*) and Glu387 and Glu206, respectively, for the latter enzyme (*40*). Moreover, Glu358 in Abg enzyme was identified as the catalytic nucleophile residue by trapping the covalent α-D-glucopyranosyl-enzyme intermediate with the mechanism-based inactivator 2′,4′-dinitrophenyl 2-deoxy-2-fluoro-β-D-glucopyranoside (2-DFG) and further determination of the labeled residue (*12*). The catalytic mechanism of Agb β-glucosidase has been extensively studied (*9*, *11*, *13*−*16*), including substrate specificity, pH dependences, kinetic isotope effects, linear free energy relationships, affinity labeling, and interaction with 2-deoxy substrates. This large body of evidence supports the oxocarbocation character of the transition state in both *glycosylation* and *deglycosylation* steps and the covalent nature of the glycosyl-enzyme intermediate, as first proposed by Koshland in the early 50's (*17*). Recently, another family 1 β-glycosidase from the hyperthermophilic *Pyrococcus furiosus* has been characterized (*18*), showing mechanistic similarities with the mesophilic homologues despite the large difference in their temperature optima. This suggested that structural modifications through evolution have maintained the integrity of the active site structure and specificity of transition state interactions while adapting the overall protein structure to function at notably different temperatures.

According to sequence similarity analysis, Bgl3 β-glucosidase has also been classified into the family 1 of glycosyl hydrolases, showing identity indexes from 35% to 55% with respect to different members of that family (*1*, *19*). The enzyme is a monomeric protein with molecular mass of 52.6 kDa and an isoelectric point of 4.4; it has a pH optimum for activity of 6.5, and the optimum temperatute for activity is 50 °C. Following sequence alignment and molecular modeling, we proposed the residues Glu383 and Glu178 as candidates to play the role of nucleophile and acid/base catalyst, respectively. In this paper we report the kinetic properties of the wild-type Bgl3 and mutants at the proposed catalytic residues with the aim of comparing the mechanistic details with other family 1 β-glucosidases and to provide further evidence on the conservation of active site structures among members of the same enzyme family according to the current classification of glycosyl hydrolases.

MATERIALS AND METHODS

Reagents and Substrates. Phenyl, 2-nitrophenyl, and 4-nitropheyl β-D-glucopyranoside and *p*-nitrophenyl β-D-glycosides of xylose, fucose, and galactose as well as all buffer chemicals were obtained from Sigma Chemical Co. 4-Bromo-, 3-nitro-, 3,5-dinitro-, 3,4-dinitro-, and 2,3-dinitrophenyl β-D-glucopyranosides were prepared by phase transfer-catalyzed glycosylation of α-bromoglucose peracetate with the corresponding phenol as reported in Dess et al. (*20*), followed by de-O-acetylation in MeONa/MeOH. 4-Methylumbelliferyl β-D-glucopyranoside was synthesized as reported in Malet et al. (*21*) and 2,4-dinitrophenyl β-D-glucopyranoside by the one-step procedure of Sharma et al. (*22*).

Cloning, Expression, and Purification of Bgl3 Enzymes from Escherichia coli. The wild-type (wt) β-glucosidase gene from *Streptomyces* sp. QM-B814, including its downstream region which may function as transcription terminator since it contains two inverted repeats (CGGTGCGGCAC and GGCCCGCCCCCG starting at 8 and 37 nucleotides from the stop codon, respectively), was cloned into the T7 polymerase expression vector pET-21d(+) (Novagen) and overexpressed in *E. coli* strain BL21(DE3) (Novagen). To simplify the protein purification protocol, a His-tag coding sequence was fused to the start codon (GTG) of the Bgl3 reading frame, obtaining the recombinant plasmid pET21-HBG3 which yields a protein with an extended N-terminus formed by the sequence MHHHHHHGIH and a deduced molecular mass of 53.6 kDa.

Each expression experiment was started by transforming competent *E. coli* BL21(DE3) cells with pET21-derived plasmids containing wt or mutant Bgl3 genes. One transformant colony grown in LB solid medium, containing ampicillin (100 μg/mL), was picked, inoculated into 3 mL of 2× YT broth + ampicillin (200 μg/mL) (*23*), and shaken overnight at 37 °C to an OD_{595} of about 0.6; aliquots of this culture were used to inoculate larger volumes of the same growth medium (usually 200 mL) that were shaken (300 rpm) for 8−10 h at 37 °C. Following such a procedure, protein expression was achieved constitutively without addition of isopropyl β-thiogalactopyranoside (IPTG). The cells were harvested and disrupted essentially according to the protocol described in the pET System Manual (Novagen); the sonication step was omitted. For protein purification, cell-free extracts were centrifuged (39000*g*, 30 min at 4 °C), and the supernatant (soluble fraction) was applied onto a 5 mL HiTrap Chelating Sepharose (Pharmacia) column previously charged with Ni^{2+} as a metal ion. Chromatography was carried out according to the manufacturer's specifications, and Bgl3-containing fractions were pooled, concentrated, and desalted by ultrafiltration at 4 °C using 50 mM sodium phosphate (pH 7.0) as desalting buffer. Using this procedure homogeneous (>99%) protein samples were obtained, as judged by SDS−polyacrylamide gel electrophoresis (SDS−PAGE) and Coomassie Brilliant Blue R-250 staining. Protein concentration was determined by the dye-binding method of Bradford (*24*) using BSA as a standard. Pure enzymes were kept at 4 °C for short periods or stored at −20 °C in the presence of 45% glycerol for prolonged periods. A protein extinction coefficient of 107 000 M^{-1} cm^{-1} at 280 nm was calculated for the wt Bgl3 according to ref *25*.

Site-Directed Mutagenesis. Different fragments cloned in pUC118, previously obtained for the *bgl3* gene sequencing (*1*), were used as templates for mutagenic polymerase chain reactions (SDM-PCR) according to the method reported by Juncosa et al. (*26*). The first PCR used the mutagenic primers and the Reverse Universal Primer flanking the 5′-end of the

bgl3 gene fragment including the target triplet. Mutagenic primers were as follows (mismatches are underlined): E383A, 5′-CTGGTCATCACCGCGAACGGCGCCGC-3′; E383Q, 5′-CGCTGGTCATCACCCAGAACGGCGCCGCC-3′;E178Q, 5′-GGACCACCCTCAACCAGCCCTGGTGCAGC-3′;E178A, 5′-GGACCACCCTCAACGCGCCCTGGTGCAGC-3′. The first PCR product was purified by agarose gel electrophoresis and used as a primer in the second PCR along with the Forward Universal Primer. Mutated fragments were purified by agarose gel electrophoresis, cloned in pUC118 vector, and completely resequenced before their substitution for the corresponding fragment in the wild-type pET21-HBG3.

Equilibrium Urea Denaturation. Unfolding of wt and mutated Bgl3 was monitored by fluorescence spectroscopy in a Perkin-Elmer LS 50 spectrofluorometer, with excitation at 280 nm (2.5 nm slit) and the emission spectra being recorded from 300 to 550 nm (4 nm slit) and measured at 340 nm, in a thermostated cuvette at 25 °C. Protein samples in 50 mM sodium phosphate buffer, pH 7.0, were diluted to a concentration of 40 μg/mL in degassed urea solutions in the same buffer and incubated 8−10 h at room temperature before fluorescence data were collected. Equilibrium denaturation data were analyzed using the Clarke and Fersht method (*27*) as previously described by Pons et al. (*28*) by fitting the fluorescence vs urea concentration data to

$$F = (a_F + b_F[\mathrm{D}] + (a_U + b_U[D]) \exp(m([\mathrm{D}] - [\mathrm{D}]_{50\%})/RT))/(1 + \exp(m([\mathrm{D}] - [\mathrm{D}]_{50\%})/RT)) \quad (1)$$

where F is the measured fluorescence, a_F and a_U are the intercepts and b_F and b_U the slopes of the baselines at low (F) and high (U) denaturant concentration, [D] is the denaturant (urea) concentration, $[D]_{50\%}$ is the concentration of denaturant at which 50% of the protein is unfolded, and m ($=\delta\Delta G_U/\delta[\mathrm{D}]$) is the slope of the transition.

Kinetic Characterization. (A) General. β-Glucosidase activity was determined by a continuous assay monitoring the release of *p*-nitrophenol from *p*-nitrophenyl β-D-glucopyranoside (pNPG) at 400 nm in a thermostated spectrophotometer. Enzyme reactions were performed in 50 mM sodium phosphate buffer, pH 6.5 or 7.0, at 50 °C using different pNPG concentrations (0.01−20 mM). The molar absorption coefficients at 400 nm ($\Delta\epsilon = \epsilon_{p-\mathrm{nitrophenol}} - \epsilon_{\mathrm{substrate}}$) were 5486 $M^{-1}\cdot cm^{-1}$ at pH 6.5 and 9510 $M^{-1}\cdot cm^{-1}$ at pH 7.0 at 50 °C. The protein concentrations in the reaction mixtures were 2−20 nM for the wild-type enzyme and 0.05−2 μM for the mutants. Rates were obtained from the initial slopes (2−5 min reaction time for the wild-type enzyme and up to 45 min for the mutants), and kinetic constants were calculated from data fitted to the Michaelis−Menten equation or to a substrate inhibition model ($v = k_{cat}[\mathrm{E}]_0[\mathrm{S}]/(K_m + [\mathrm{S}] + [\mathrm{S}]^2/K_i)$) by means of nonlinear regression analysis. Activity against other *p*-nitrophenyl sugars was analyzed following the assay described above.

(B) pH Profile. The pH dependence of enzyme activity was studied using pNPG (0.5 mM) as a substrate in 50 mM phosphate buffer, $I = 0.15$ M with added KCl, at 40 °C. The stability of the enzyme at each pH was first determined, and activity was calculated at pH values at which the enzyme was stable for at least 5 min. The pH-dependent molar extinction coefficients of *p*-nitrophenol at 378 nm (for reaction at pH ≤5.5) and 400 nm (for reactions at pH >5.5) were accurately measured at the conditions used for the kinetic assays. Values of ϵ_{378} and ϵ_{400} at different pH values were fitted by nonlinear regression to the equation

$$\epsilon_{\mathrm{pNP-OH},\lambda} = (\epsilon_{\mathrm{NPH},\lambda} + \epsilon_{\mathrm{NP}^-,\lambda} \times 10^{\mathrm{pH}-\mathrm{p}K_a})/(1 + 10^{\mathrm{pH}-\mathrm{p}K_a}) \quad (2)$$

where NPH and NP^- are the un-ionized and ionized forms of *p*-nitrophenol, respectively, and $\epsilon_{\mathrm{pNP-OH},\lambda}$ is the measured molar extintion coeficient at each λ. The adjusted parameters were $\epsilon_{\mathrm{NPH},378} = 992\ M^{-1}\ cm^{-1}$, $\epsilon_{\mathrm{NP}^-,378} = 13\,695\ M^{-1}\ cm^{-1}$, $\epsilon_{\mathrm{NPH},400} = 114\ M^{-1}\ cm^{-1}$, $\epsilon_{\mathrm{NP}^-,378} = 18\,131\ M^{-1}cm^{-1}$, and $pK_a = 6.92$.

(C) Hammett Analysis. Kinetic constants for the enzyme-catalyzed hydrolysis of a series of aryl β-D-glucosides were determined by measuring the release of the aglycon by UV spectrophotometry in 50 mM phosphate buffer, pH 6.5, $I = 0.15$ M with added KCl, at 30 °C. Molar extinction coefficients of the aryl β-glucosides and the aglycons (free phenols) were determined at the appropriate wavelength under the same conditions [wavelength and $\Delta\epsilon$ ($=\epsilon_{\mathrm{phenol}} - \epsilon_{\mathrm{substrate}}$) are listed in Table 3].

(D) Chemical Rescue. Kinetics of wt and mutant enzymes in the presence of sodium azide (0−100 mM) were evaluated for *p*-nitrophenyl β-D-glucopyranoside (pNPG) and 2,4-dinitrophenyl β-D-glucopyranoside (2,4-DNPG)[1] substrates by monitoring the release of the phenol aglycon in 50 mM phosphate buffer, pH 6.5, at 50 °C for pNPG ($\lambda = 400$ nm, $\Delta\epsilon = 5486\ M^{-1}\ s^{-1}$), and 30 °C for 2,4-DNPG ($\lambda = 400$ nm, $\Delta\epsilon = 2178\ M^{-1}\ s^{-1}$). Substrate and enzyme concentrations are given in Table 4.

(E) NMR Monitoring. ^{1}H NMR monitoring of enzymatic reactions was performed following the procedure reported in Viladot et al. (*29*) on a Varian Gemini 300 spectrometer at 30 °C in 9 mM sodium phosphate buffer at pD 7.0 (adjusted with 1 N NaOD/D_2O). Spectra were recorded at intervals of 15 min during a total time of 10−24 h. Enzyme and nucleophile concentrations were (a) E178A [enzyme] = 300 nM, [azide] = 100 mM, [substrate] = 3.75 mM and (b) E383A [enzyme] = 800 nM, [azide] = 200 mM, [substrate] = 3.2 mM.

RESULTS AND DISCUSSION

Mutagenesis and Expression. To undertake both mutational and structural studies with the Bgl3 glucosidase, the availability of a quick protein expression and purification procedure was the first pitfall to be overcome. The Bgl3 encoding gene was initially cloned in *Streptomyces lividans* where it expresses intracellularly from the own promoter (*1*); such a promoter is not functional in *E. coli*. Moreover, pure enzyme preparations from the streptomycete host involve from three to seven purification steps, depending on the volume of culture processed, with the concomitant decrease in protein yields. Thus, a series of attempts to express Bgl3

[1] Abbreviations: pNPGal, *p*-nitrophenyl β-D-galactoside; pNGlu, *p*-nitrophenyl β-D-glucoside; pNPFuc, *p*-nitrophenyl β-D-fucoside; pNPXyl, *p*-nitrophenyl β-D-xyloside; PG, phenyl β-D-glucoside; 4-BrPG, 4-bromophenyl β-D-glucoside; 3-NPG, 3-nitrophenyl β-D-glucoside; MUG, 4-methylumbelliferyl β-D-glucoside; 2-NPG, 2-nitrophenyl β-D-glucoside; 4-NPG or pNPG, 4-nitrophenyl β-D-glucoside; 3,5-DNPG, 3,5-dinitrophenyl β-D-glucoside; 3,4-DNPG, 3,4-dinitrophenyl β-D-glucoside; 2,3-DNPG, 2,3-dinitrophenyl β-D-glucoside; 2,4-DNPG, 2,4-dinitrophenyl β-D-glucoside.

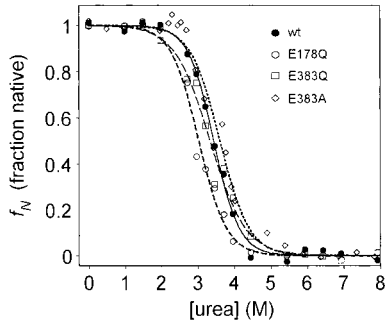

FIGURE 1: Equilibrium urea denaturation curves for the wild-type and mutant β-glucosidases. Fluorescence intensity values were fitted to eq 1, and the adjusted parameters are given in Table 1. Normalized curves are plotted as the fraction native $f_N = (F - (a_U + b_U[D]))/(a_F - a_U + [D](b_F - b_U))$, where F is the measured fluorescence intensity and a_U, a_F, b_U, and b_F are the adjusted parameters from eq 1.

in *E. coli* were carried out, including extracellular expression by fusion to several signal peptides from *E. coli* and *Bacillus licheniformis*. Among other vectors successfully tested [i.e., pUCBM21 (Boehringer Mannheim) expressing Bgl3 from *lac* promoter], the pET system (Novagen) and N-terminal fusion of a His tag have allowed to obtain very high yields of soluble enzyme (150−200 mg/L of *E. coli* culture) following a one-step purification protocol. In contrast, the His-tag fusion to the C-terminal end of Bgl3 glucosidase was absolutely deleterious for its expression in a soluble form as was any attempt of secretion by fusing different signal peptides to the N-terminal end. The recombinant Bgl3 carrying the N-terminal extension (see Materials and Methods) obtained from *E. coli* did not differ significantly from the enzyme purified from *S. lividans* comparing activity−pH profiles, substrate specificity, kinetic constants, and thermostability (not shown).

The choice of the amino acid residues essential for catalysis was based on sequence alignment between Bgl3 and different members of family 1 glycosyl hydrolases, taking into account that glutamic acid residues 358 and 170 had been previosly identified as the nucleophile and general acid/base catalyst, respectively, in the Abg enzyme (*10*−*12*). The corresponding residues in Bgl3 are Glu383 and Glu178, which are found in the highly conserved motifs I-T-E-N-G-A and N-E-P-W, respectively. On the basis of the first 3D structure of a glucosidase belonging to the family 1 glycosyl hydrolases (*30*), a model structure of Bgl3 was obtained and used to verify the positioning of the residues chosen upon alignment. On the modeled structure, the putative role of Glu383 and Glu178 residues was reinforced, being located in the inner region of the active site pocket and presenting a distance of about 0.4 nm between their respective carboxylate groups.

Glu383 and Glu178 were substituted by the isosteric glutamine (charge removal) and by alanine (side chain and charge removal). The mutant Bgl3 enzymes were obtained by site-directed mutagenesis and expressed and purified following the procedure described for the wild type.

Unfolding. To ascribe the changes in kinetic behavior to the introduced mutations, the proper folding or stability of the mutants was evaluated by equilibrium urea denaturation. Thus, unfolding was monitored by measuring the dependence of fluorescence intensity on urea concentration (Figure 1) and fitting the fluorescence vs urea concentration to eq 1 (Table 1). Considering that $[D]_{50\%}$ is the concentration of denaturant at which 50% of the protein is unfolded, the mean $[D]_{50\%}$ value between mutant enzymes, as calculated from the fluorescence curves, was 3.3 M urea (with a standard deviation of ±0.3). Such a value compares well with $[D]_{50\%}$ calculated for wild-type Bgl3, i.e., 3.44 M urea, as do the denaturation curves from 0 to 8 M urea (Figure 1). These results support a folded structure for the mutant proteins, and hence, changes of the catalytic properties can be assigned to the replacement of the target amino acid residues.

Table 1: Equilibrium Urea Denaturation Data for wt and Mutant β-Glucosidases[a]

mutant	M (kcal·mol^{-1}·M^{-1})	$[D]_{50\%}$ (M)	ΔG^{H_2O} [b] (kcal·mol^{-1})
wild type	1.69	3.44 ± 0.02	5.8
E178Q	1.56	3.03 ± 0.04	4.7
E383Q	1.23	3.34 ± 0.04	4.1
E383A	1.48	3.61 ± 0.04	5.3

[a] Conditions: 50 mM phosphate, pH 7.0, 0−8 M urea, 40 μg/mL enzyme. [b] $\Delta G^{H_2O} = m[D]_{50\%}$.

Table 2: Michaelis−Menten Parameters of *Streptomyces* sp. β-Glucosidases (wt and Mutants) with Cellobiose and *p*-Nitrophenyl β-Glycoside Substrates[a]

mutant	substrate	K_M (mM)	k_{cat} (s^{-1})	k_{cat}/K_M (M^{-1} s^{-1})
wt	cellobiose	4.1	35.6	8.60×10^3
	PNPGlu	0.15	28.4	1.90×10^5
	PNPFuc	0.14	37.1	2.65×10^5
	PNPGal	7.3	118	1.61×10^4
	PNPXil	3.0	0.63	2.11×10^2
E178Q	PNPGlu	0.02	0.015	7.77×10^2
	PNPFuc	0.11	1.08	9.90×10^3
	PNPGal	4.5	0.66	1.50×10^2
E178A	PNPGlu	0.65	0.036	5.52×10^1
	PNPFuc	0.22	0.011	4.86×10^1
	PNPGal	0.12	0.004	3.65×10^1
E383Q	PNPGlu	0.20	$\approx 3 \times 10^{-5}$	1.6×10^{-1}
	PNPFuc	0.26	$\approx 2 \times 10^{-5}$	6.0×10^{-2}
	PNPGal	0.04	$\approx 1 \times 10^{-4}$	4.0
E383A	PNPGlu	0.03	$\approx 4 \times 10^{-5}$	1.4
	PNPFuc	0.23	$\approx 2 \times 10^{-4}$	9.2×10^{-1}
	PNPGal	0.04	$\approx 8 \times 10^{-4}$	2.0×10^1

[a] Conditions: 50 mM phosphate buffer, pH 6.5, 50 °C (for wt, E178Q, and E178A), pH 7.0, 30 °C (for E383Q and E383A), [enzyme] = 0.02 μM (wt), 0.075−0.2 μM (E178Q), 0.048−0.28 μM (E178A), 1.18 μM (E383Q), and 0.54 μM (E383A). Protein concentrations were determined by the Bradford assay using BSA as a standard.

Substrate Specificity. Kinetics for the wild-type and mutant β-glucosidases were evaluated with different *p*-nitrophenyl β-glycosides as summarized in Table 2. The wt enzyme has a broad substrate specificity which is common among glycosyl hydrolases from family 1, such as β-glucosidases from *Agrobacterium faecalis* (*13*), *Bacillus polymyxa* (*31*), *Thermotoga maritima* (*32*), *Sulfolobus solfataricus* (*33*), and *Pyrococcus furiosus* (*18*). Glucoside and fucoside substrates show the highest catalytic efficiency (in terms of k_{cat}/K_M), but a significant substrate inhibition is obtained for the *p*-nitrophenyl β-glucoside as opposed to the fucoside (Figure 2). The k_{cat} value for the galactoside (pNPGal) substrate is 4-fold higher than that for the glucoside (pNPGlu), but the lower K_M for the latter results in an overall 10-fold glucosidase over galactosidase activity in terms of k_{cat}/K_M.

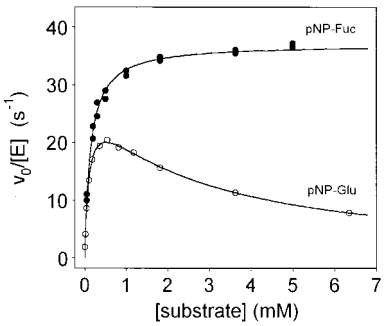

FIGURE 2: Steady-state kinetics for the enzyme-catalyzed hydrolysis of *p*-nitrophenyl β-D-glucoside (pNPGlu) and *p*-nitrophenyl β-L-fucoside (pNPFuc) at 50 °C in 50 mM phosphate buffer, pH 6.5.

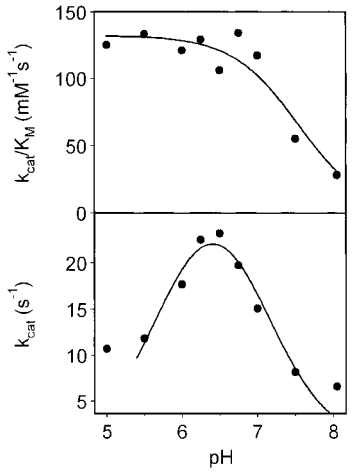

FIGURE 3: pH dependence of the kinetic parameters of wild-type *Streptomyces* sp. β-glucosidase with *p*-nitrophenyl β-D-glucoside: (a, bottom) pH profile of k_{cat}; (b, top) pH profile of k_{cat}/K_M.

The lowest efficiency among the substrates assayed corresponds to the xyloside (pNPXyl) with a 1000-fold decrease in k_{cat}/K_M as compared to the pNPGlu substrate, indicating that the interactions between the 5-hydroxymethyl group and the binding pocket of the enzyme have a stabilizing effect on the transition state. The magnitude of this interaction can be estimated according to (*18*, *34*)

$$\Delta\Delta G^{\ddagger} = -RT \ln[(k_{cat}/K_M)_{xyl}/(k_{cat}/K_M)_{glu}] \qquad (3)$$

where $\Delta\Delta G^{\ddagger}$ is the change in the activation free energy between both substrates and $(k_{cat}/K_M)_{xyl}$ and $(k_{cat}/K_M)_{glu}$ are the catalytic efficiencies for the pNPXyl and pNPGlu substrates, respectively. A value of 18.5 kJ·mol^{-1} is lost upon removal of the 5-hydroxymethyl group, comparable to the 16.3 kJ·mol^{-1} for the *A. faecalis* (*13*) and the 10 kJ·mol^{-1} for the *P. furiosus* (*18*) β-glucosidases.

pH and Temperature Dependence. The steady-state values of k_{cat}, K_M, and k_{cat}/K_M for the β-glucosidase-catalyzed reaction of pNPGlu were measured over the pH range of 5−8 at 40 °C and constant ionic strength (0.15 M) (Figure 3). The pH dependence of k_{cat} follows a double ionization curve, with kinetic pK_a values of aproximately 5.7 and 7.1. k_{cat} parameters at low and high pH could not be accurately measured due to large increases in K_M values. Moreover, enzyme precipitation was apparent at pH <5. In the pH range studied, a single ionization curve was obtained for k_{cat}/K_M, with a kinetic pK_a in the basic limb of 7.5. Since the pH profile on k_{cat}/K_M reflects ionization constants in the free enzyme, and on k_{cat} in the E·S complex, the low pK_a in the free enzyme (not observed in the k_{cat}/K_M plot) should be below 5, which is shifted to 5.7 in the E·S complex. On the other hand, catalysis depends on a protonated group with a pK_a of 7.1−7.5 (on the E·S complex and free enzyme, respectively). Comparison with other family 1 β-glucosidases shows a similar behavior, mainly for the protonated group with high pK_a: 7.0−7.4 for the *P. furiosus* β-glucosidase (*18*) and 7.6−8.1 for the *A. faecalis* enzyme (*13*), indicating that the specific hydrogen bonds that occur between the catalytic amino acids and other active site residues are similar in these enzymes.

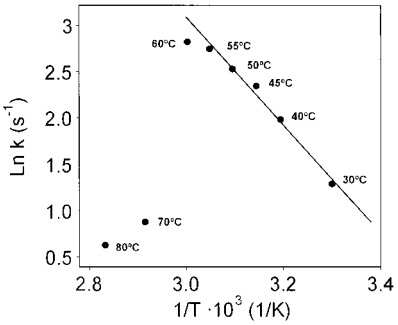

FIGURE 4: Temperature dependence of the β-glucosidase activity on *p*-nitrophenyl β-D-glucoside substrate in 50 mM phosphate buffer, pH 6.5, [pNPGlu] = 588 μM, [enzyme] = 5.6 nM, and temperature range 30−80 °C.

The *Streptomyces* β-glucosidase shows a linear Arrhenius plot for the reaction with the pNPGlu substrate in the temperature range from 30 to 55 °C (Figure 4). The calculated activation energy (E_a) of 49.9 kJ·mol^{-1} is of the same magnitude than those determined for other family 1 β-glucosidases (*18*). At temperatures higher than 60 °C, the enzyme is rapidly inactivated.

Enzyme Mechanism: Structure−Reactivity Studies. As a retaining glycosidase, the mechanism of Bgl3 involves a two-step process (*5*, *6*). In the first step (*glycosylation*) the amino acid residue acting as a general acid protonates the glycosidic oxygen with concomitant C−O breaking of the scissile glycosidic bond, while the deprotonated carboxylate functioning as a nucleophile attacks the anomeric center to give a covalent glycosyl-enzyme intermediate (E−G). The second *deglycosylation* step involves the attack of a water molecule assisted by the conjugate base of the general acid to render the free sugar with overall retention of configuration (G−OH). Both steps proceed via transition states with considerable oxocarbenium ion character.

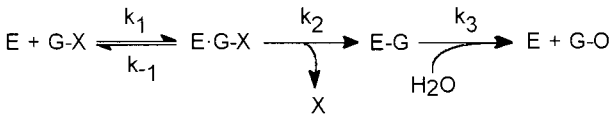

In this mechanism, $k_{cat} = k_2k_3/(k_2 + k_3)$, $K_M = k_3(k_2 + k_{-1})/k_1(k_3 + k_2)$, and $k_{cat}/K_M = k_1k_2/(k_2 + k_{-1})$.

A series of substituted aryl β-glucosides were used as substrates of the β-glucosidase-catalyzed reaction to evaluate the effect of the aglycon leaving group on reaction rates. Kinetic data are presented in Table 3. All substrates showed substrate inhibition at high substrate concentration, and k_{cat} and K_M values were obtained by fitting the initial velocities vs substrate concentration to the Michaelis−Menten equation

Table 3: Kinetic Parameters of Aryl β-D-Glucosides with *Streptomyces* sp. β-Glucosidase at 30 °C[a]

substrate	concn range (mM)	$\Delta\epsilon$ ($M^{-1}\cdot cm^{-1}$) [λ (nm)][b]	pK_a (phenol)	k_{cat} (s^{-1})	K_M (mM)	K_I (mM)	k_{cat}/K_M ($M^{-1}\cdot s^{-1}$)
PG	0.04−9.3	1414 [270]	9.99	0.66 ± 0.08	2.3 ± 0.4	16 ± 7	2.83×10^2
4-BrPG	0.06−4.8	909 [288]	9.34	3.32 ± 0.12	0.47 ± 0.03	28 ± 10	7.11×10^3
3-NPG	0.01−1.6	224 [385]	8.39	15.8 ± 2.10	0.24 ± 0.05	1.2 ± 0.3	6.52×10^4
MUG	0.001−1.3	1986 [355]	7.53	11.7 ± 0.30	0.058 ± 0.004	4.6 ± 0.8	2.04×10^5
2-NPG	0.002−1.0	1459 [379]	7.22	7.72 ± 0.90	0.023 ± 0.017	0.18 ± 0.05	3.43×10^5
4-NPG	0.002−1.7	5088 [400]	7.18	8.14 ± 0.40	0.10 ± 0.01	1.4 ± 0.1	7.85×10^4
3,5-DNPG	0.01−1.8	87 [400]	6.69	20.5 ± 0.70	0.054 ± 0.005	11 ± 4	3.78×10^5
3,4-DNPG	0.003−1.2	8953 [400]	5.36	18.2 ± 1.0	0.064 ± 0.007	6.4 ± 0.6	2.87×10^5
2,3-DNPG	0.003−0.4	2475 [420]	4.96	11.7 ± 0.7	0.015 ± 0.002	2.1 ± 1.5	7.70×10^5
2,4-DNPG	0.001−0.1	2178 [400]	3.96	30.4 ± 1.0	0.008 ± 0.001	0.23 ± 0.04	3.83×10^6

[a] Conditions: 50 mM phosphate buffer, pH 6.5, $I = 0.15$ M with added KCl, 30 °C. [b] λ, wavelength at which the release of the aglycon was monitored spectrophotometrically; $\Delta\epsilon$ values ($=\epsilon_{phenol} - \epsilon_{substrate}$) were determined at the given wavelength in the same buffer and temperature used in the kinetic runs. Protein concentrations were determined by the Bradford assay using BSA as a standard.

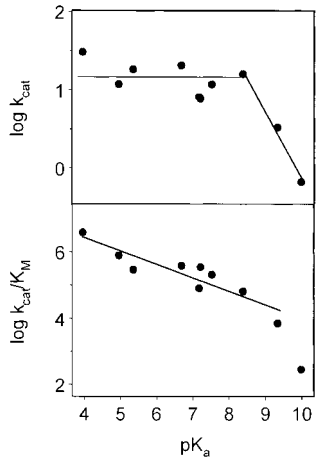

FIGURE 5: Hammett relationship for the β-glucosidase-catalyzed hydrolysis of aryl β-glucosides. Data are presented in the form of a Brønsted plot (log k_{cat} versus pK_a of the aglycon phenol). Kinetic data and experimental conditions are given in Table 3.

with substrate inhibition model. The effect of substrate reactivities on k_{cat} and k_{cat}/K_M was evaluated by means of a Hammett analysis, the electronic effects of the phenol substituents being expressed as the pK_a of the free phenol released upon enzymatic hydrolysis. Therefore, the Hammett equation is written in the form of the Brønsted equation

$$\log k = \text{constant} + \beta_{lg} pK_a$$

where k is k_{cat} or k_{cat}/K_M and β_{lg} is the reaction constant reflecting the sensitivity of the reaction to the electronic effect of the substituents. The Hammett relationships between reaction rates and leaving group ability (as pK_a of the phenols) are presented in Figure 5. A biphasic plot of log k_{cat} vs pK_a was obtained, which corresponds to a change in the rate-determining step from less reactive to more reactive substrates. The plot is linear with a slope (Brønsted coefficient β_{lg}) of −0.8 for substrates with poor leaving ability (pK_a > 8), indicating that the first *glycosylation* step is rate limiting and k_{cat} is proportional to the reactivity of the substrate. Glycosides with good leaving groups (pK_a < 8) show no significant dependence of log k_{cat} on pK_a, the aglycon-independent *deglycosylation* step now being rate limiting. This biphasic behavior is similar to that observed for the *A. faecalis* and *P. furiosus* β-glucosidases (*13*, *18*), with close reaction constants ($\beta_{1g} = -0.7$) for the less reactive substrates; the formation of the glycosyl-enzyme intermediate is rate limiting, and there is a large degree of bond cleavage with charge development at the transition state for substrates with poor leaving groups, whereas hydrolysis of the glycosyl-enzyme intermediate becomes rate limiting for activated substrates.

The Hammett plot for the second-order rate constant k_{cat}/K_M (Figure 5) is linear and also shows a concave downward curvature at high pK_a values. Since k_{cat}/K_M contains rate constants up to the first irreversible step (which is *glycosylation*), the curvature cannot be related to a change in rate-limiting *glycosylation* to *deglycosylation*, but rather it may reflect a change in the rate of enzyme−substrate association (k_1) relative to the rate of *glycosylation* (k_2).

Catalytic Residues. Mutation of the proposed catalytic residues, Glu178 and Glu383, to Gln and Ala yields less active to inactive enzymes (Table 2). For the Glu178 residue, assigned to the general acid/base on the basis of sequence similarities, mutation to Gln gave a 250-fold reduction of k_{cat}/K_M (pNPGlu substrate), whereas mutation to Ala produced a 3500-fold decrease in catalytic efficiency. Larger effects are obtained for mutants at Glu383, proposed as the catalytic nucleophile, with 10^6-10^5-fold reductions in k_{cat}/K_M for the E383Q and E383A mutants.

Chemical Rescue of Inactive Mutants. The functional role of both residues in the enzyme mechanism was assessed by a chemical rescue methodology with an exogenous nucleophile as applied to a number of glycosidases [i.e., β-glucosidases (*11*, *35*, *36*), 1,4-β-exoglucanase (*37*), 1,3-1,4-β-glucanase (*29*, *38*), β-galactosidase (*39*)]. For a retaining β-glycosidase, removal of the general acid/base residue will have little or no effect on the first *glycosylation* step for an activated substrate (2,4-DNP glycoside) that does not require general acid assistance, but the reaction will stop at the *deglycosylation* step. The glycosyl-enzyme intermediate will be slowly hydrolyzed in the absence of the general base to assist the attack of a water molecule. Addition of an exogenous nucleophile (such as azide) that does not require general base assistance may attack the glycosyl-enzyme intermediate instead of a water molecule with the overall effect of enzyme reactivation. Since the exogenous nucleophile will operate on the *deglycosylation* step, the reaction will yield the β-glycosyl product. On the other hand, mutation of the nucleophile should render an inactive mutant where the first *glycosylation* step has been drastically slowed because of the absence of the nucleophilic residue to form the glycosyl-enzyme intermediate. In this case, a cavity has

Table 4: Kinetic Parameters for Wild-Type and Mutant *Streptomyces* sp. β-Glucosidases in the Absence and Presence of Sodium Azide (Chemical Rescue of Inactive Mutants)[a]

substrate	enzyme	azide (mM)	K_M (μM)	k_{cat} (s^{-1})	k_{cat}/K_M ($M^{-1}\,s^{-1}$)
pNPG	wt		150	28.4	1.90×10^5
	E178A	0	648	0.036	5.52×10^1
		50	1436	0.12	8.18×10^1
	E178Q	0	19.7	0.015	7.77×10^2
		50	575	1.38	2.40×10^3
	E383A[b]	0	26	$\approx 4 \times 10^{-5}$	1.4
		255	36	$\approx 4 \times 10^{-5}$	1.1
2,4-DNPG	wt		8.0	30.4	3.83×10^6
	E178A	0	0.3	0.022	7.4×10^4
		50	1.8	4.14	2.3×10^6
	E178Q	0	5.4	0.076	1.4×10^4
		50	3.2	2.04	6.4×10^5
	E383A	0	27	3.5×10^{-4}	1.3×10^1
		255	168	3.1×10^{-3}	1.9×10^1
		1000	990	4.7×10^{-2}	4.8×10^1

[a] Conditions: 50 mM phosphate buffer, pH 6.5, $I = 0.15$ M with added KCl, 50 °C (for pNPG substrate), 30 °C (for 2,4-DPNG substrate). [b] Parameters determined at 30 °C, pH 7.0. Protein concentrations were determined by the Bradford assay using BSA as a standard.

been created in the active site on the α-face (Glu to Ala mutation) which can accommodate a small exogenous nucleophile such as azide. The enzyme might be reactivated through a different mechanism, following a single inverting displacement to give the α-glycosyl product. Therefore, if reactivation occurs, the stereochemistry of the new glycosyl azide product formed upon chemical rescue of both alanine mutants will indicate which residue acts as the general acid/base and which operates as the nucleophile in the catalytic mechanism of the wild-type enzyme.

Addition of sodium azide as exogenous nucleophile to the reaction of the inactive alanine mutants at each catalytic residue with an activated substrate (2,4-DPNGlu) restored enzyme activity. The enzymatic reactions were monitored by ^{1}H NMR spectroscopy (in D_2O at pD 7.0 and 30 °C) for structure determination of the final products. The reactions took 1−3 days to completeness at the low enzyme concentrations used in the assays. The reaction of E178A in the presence of 100 mM azide yielded the β-glucosyl azide product: a doublet at δ 4.75 ppm ($J = 8$ Hz), which corresponds to H-1 of the β-anomer, develops at the same rate at which the doublet corresponding to H-1 of the substrate (δ 5.45 ppm, $J = 7.5$ Hz) disappears. No hydrolysis products are detected when the final spectrum is compared to that of the wild-type reaction with the same substrate, where the β (δ 4.66 ppm) and α (δ 5.23 ppm) anomers of glucose (hydrolysis product) are formed. On the other hand, time course monitoring of the reaction of E383A + 200 mM azide reveals the formation of a doublet at δ 5.55 ppm ($J =$ 3.6 Hz), assigned to H-1 of the α-glucosyl azide product, which parallels the disappearance of the doublet at δ 5.45 ppm ($J = 7.5$ Hz) of the 2,4-DPNG substrate. Both reactions are complete, and the azide adducts formed are stable after long incubation times. On the basis of the rationale of the chemical rescue methodology, these results provide functional evidence of Glu178 as being the general acid/base residue and Glu383 the catalytic nucleophile.

Kinetics of enzyme reactivation for the E178A, E178Q, and E383A mutants are summarized in Table 4. For the

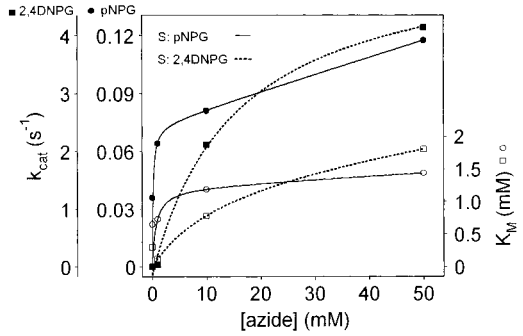

FIGURE 6: Kinetics of chemical rescue of the E178A mutant by sodium azide with pNPG (solid line) and 2,4-DPNG (dotted line) substrates. Solid symbols are for k_{cat} values and open symbols for K_M values.

E178A mutant with pNPG substrate, just a 3-fold increase in k_{cat} is observed upon addition of 50 mM sodium azide, whereas a 200-fold increase is obtained with the more activated 2,4-DPNG substrate. As shown in Figure 6, K_M values also follow an increase with azide concentration that parallels the effect on k_{cat}, thus keeping k_{cat}/K_M approximately constant. Since k_{cat}/K_M reflect the first irreversible step, most probably the glycosydation step to form the glycosyl-enzyme intermediate, its constant value across the range of azide concentrations studied is consistent with the effect of the azide anion as a nucleophile primarily on the deglycosylation step and not on glycosylation. Likewise, the increase in K_M values with increasing azide is a consequence of the relative decrease of the amount of accumulated intermediate as the deglycosylation step speeds up.

The kinetic behavior of chemical rescue obtained for the Bgl3 enzyme is similar to that reported for the exoglucanase/xylanase Cex from *Cellulomonas fimi* (*37*): the activity of the Ala mutant at the general acid/base residue with an activated substrate (2,4-dinitrophenyl β-glycoside) was restored by addition of azide and also, although to a lesser extent, with a less activated *p*-nitrophenyl glycoside substrate, consistent with *deglycosylation* being rate determining for both substrates. For the Abg β-glucosidase from *Agrobacterium* (*11*), the corresponding mutant E170G is reactivated with the 2,4-DPNG substrate, but not with pNPG, for which *glycosylation* was rate limiting, whereas rate-determining *deglycosylation* operated on the 2,4-DPNG substrate. The low but significant reactivation of the Bgl3 E178A mutant here reported with pNPG indicates that for this substrate the *deglycosylation* step is still partially rate determining, and it becomes fully rate determining for the more activated 2,4-DPNG where a larger reactivation by azide is obtained. Regardless of the small differences, these systems have in common that azide operates on the *deglycosylation* step since k_{cat}/K_M values are kept approximately constant on azide concentration. However, it seems not to be general for other retaining glycosidases as shown, i.e., for the *B. licheniformis* 1,3-1,4-β-glucanase (*29*) where k_{cat} increases (activation) but K_M values decrease with azide concentration, indicating that the exogenous nucleophile not only reactivates the mutant enzyme at the general acid/base residue as nucleophile in the *deglycosylation* step but also has an effect on the *glycosylation* step.

The nucleophile-less E383A mutant of Bgl3 shows no significant reactivation by azide with pNPG substrate (Table

4), indicating that the *p*-nitrophenol aglycon is not a good enough leaving group for the single displacement reaction to give the α-glucosyl azide product. With the more activated 2,4-DNPG substrate, the steady-state activity is partially restored, with a 100-fold increase in k_{cat} and also an increase in K_M at 1 M azide concentration.

CONCLUSIONS

As a member of glycosyl hydrolases family 1, the *β*-glucosidase Bgl3 from *Streptomyces* shares similar mechanistic and kinetic properties with other family 1 *β*-glucosidases either from mesophiles [i.e., Agb from *Agrobacterium* (*13*)] or from thermophiles [i.e., Bgl from *Pyrococcus* (*18*)]. Substrate specificity, however, reveals that the Bgl3 enzyme is highly active on fucosyl glycosides, for which no substrate inhibition is observed as opposed to the glucosyl, galactosyl, and xylosyl glycoside substrates. Reactivity studies on the wt enzyme with aryl *β*-glucosides indicate that the glycosylation step is rate determining for the less reactive substrate (pK_a of the phenol leaving group > 8) whereas deglycosylation becomes rate determining for more reactive substrates.

The identity of the catalytic residues, initially inferred from sequence alignments with other well-known *β*-glucosidases, has been confirmed by site-directed mutagenesis (Glu to Gln and Ala mutations) and their role in catalysis assessed by chemical rescue of the inactive alanine mutants at each residue with addition of azide as the exogenous nucleophile. In conclusion, Glu178 is the general acid/base residue, and Glu383 acts as the catalytic nucleophile in the retaining mechanims of Bgl3. Kinetics of mutant (E178A) reactivation by azide reveal subtle differences with other glycosidases, which together with the different substrate inhibition shown by the wt enzyme, indicate that there are subtle differences in the fine-tuning of the enzyme activity but that family 1 *β*-glucosidases share similar catalytic properties.

REFERENCES

1. Perez-Pons, J. A., Cayetano, A., Rebordosa, X., Lloberas, J., Guasch, A., and Querol, E. (1994) *Eur. J. Biochem. 223*, 557−565.
2. Montero, E. (1998) Ph.D. Thesis, Universidad Complutense de Madrid.
3. Montero, E., Vallmitjana, M., Pérez-Pons, J. A., Querol, E., Jiménez-Barbero, J., and Cañada, F. J. (1998) *FEBS Lett. 421*, 243−248.
4. Guasch, A., Vallmitjana, M., Pérez, R., Querol, E., Pérez-Pons, J. A., and Coll, M. (1999) *Acta Crystallogr., Sect. D: Biol. Crystallogr. 55*, 679−682.
5. Sinnott, M. L. (1990) *Chem. Rev. 90*, 1171−1202.
6. Davies, G., Sinnott, M. L., and Withers, S. G. (1998) in *Comprehensive Biological Catalysis* (Sinnott, M. L., Ed.) pp 119−209, Academic Press Ltd., London.
7. Heightman, T. D., and Vasella, A. (1999) *Angew. Chem., Int. Ed. Engl. 38*, 750−770.
8. Henrissat, B., and Bairoch, A. (1993) *Biochem. J. 293*, 781−788.
9. McCarter, J. D., and Withers, S. G. (1994) *Curr. Opin. Struct. Biol. 4*, 885−892.
10. Trimbur, D. E., Warren, R. A. J., and Withers, S. G. (1992) *J. Biol. Chem. 267*, 10248−10251.
11. Wang, Q., Trimbur, D. E., Graham, R., Warren, R. A. J., and Withers, S. G. (1995) *Biochemistry 34*, 14554−14562.
12. Withers, S. G., Warren, R. A. J., Street, I. P., Rupitz, K., Kempton, J. B., and Aebersold, R. (1990) *J. Am. Chem. Soc. 112*, 5887−5889.
13. Kempton, J. B., and Withers, S. G. (1992) *Biochemistry 31*, 9961−9969.
14. Street, I. P., Kempton, J. B., and Withers, S. G. (1992) *Biochemistry 31*, 9970−9978.
15. Namchuk, M. N., and Withers, S. G. (1995) *Biochemistry 34*, 16194−16202.
16. Withers, S. G. (1995) in *Carbohydrate Bioengineering* (Petersen, S. B., Svensson, B., and Pedersen, S., Eds.) pp 97−111, Elsevier, Amsterdam.
17. Koshland, D. E., Jr. (1953) *Biol. Rev. 28*, 416−436.
18. Bauer, M. W., and Kelly, R. M. (1998) *Biochemistry 37*, 17170−17178.
19. Perez-Pons, J. A., Padros, E., and Querol, E. (1995) *Biochem. J. 308*, 791−794.
20. Dess, D., Kleine, H. P., Weinberg, D. V., Kaufman, R. J., and Sidhu, R. S. (1981) *Synthesis*, 883−885.
21. Malet, C., Viladot, J. L., Ochoa, A., Gállego, B., Brosa, C., and Planas, A. (1995) *Carbohydr. Res. 274*, 285−301.
22. Sharma, S. K., Corrales, G., and Penades, S. (1995) *Tetrahedron Lett. 36*, 5627−5630.
23. Sambrook, J., Fritsch, E. F., and Maniatis, T. (1989) *Molecular cloning: a laboratory manual*, Cold Spring Harbor Laboratory, Cold Spring Harbor, NY.
24. Bradford, M. M. (1976) *Anal. Biochem. 72*, 248−254.
25. Gill, S. C., and van Hippel, P. H. (1989) *Anal. Biochem. 182*, 319−326.
26. Juncosa, M., Pons, J., Dot, T., Querol, E., and Planas, A. (1994) *J. Biol. Chem. 269*, 14530−14535.
27. Clarke, J., and Fersht, A. R. (1993) *Biochemistry 32*, 4322−4329.
28. Pons, J., Planas, A., and Querol, E. (1995) *Protein Eng. 8*, 939−945.
29. Viladot, J. L., de Ramon, E., Durany, O., and Planas, A. (1998) *Biochemistry 37*, 11332−11342.
30. Barrett, T., Suresh, C. G., Tolley, S. P., Dodson, E. J., and Hughes, M. A. (1995) *Structure 3*, 951−960.
31. Painbeni, E., Valles, S., Polaina, J., and Flors, A. (1992) *J. Bacteriol. 174*, 3087−3091.
32. Gabelsberger, J., Liebl, W., and Schleifer, K.-H. (1993) *FEMS Microbiol. Lett. 109*, 131−138.
33. Nucci, R., Moracci, M., Vaccaro, C., Vespa, N., and Rossi, M. (1993) *Biotechnol. Appl. Biochem. 17*, 239−250.
34. Fersht, A. R. (1988) *Biochemistry 27*, 1577−1580.
35. Wang, Q., Graham, R. W., Trimbur, D. E., Warren, R. A. J., and Withers, S. G. (1994) *J. Am. Chem. Soc. 116*, 11594−11595.
36. Moracci, M., Trincone, A., Perugino, G., Ciaramella, M., and Rossi, M. (1998) *Biochemistry 37*, 17262−17270.
37. Macleod, A. M., Lindhorst, T., Withers, S. G., and Warren, R. A. J. (1994) *Biochemistry 33*, 6371−6376.
38. Planas, A. (1998) in *Carbohydrases from Trichoderma reesei and other microorganisms* (Claeyssens, M., Nerinckx, W., and Piens, K., Eds.) pp 21−38, The Royal Society of Chemistry, Cambridge.
39. Richard, J. P., Huber, R. E., Lin, S., Heo, C., and Amyes, T. L. (1996) *Biochemistry 35*, 12377−12386.
40. Moracci, M., Capalbo, L., Ciaramella, M., and Rossi, M. (1996) *Protein Eng. 9*, 1191−1195.

BI002947J